# Mechanism of Nonphotochemical Quenching in Green Plants: Energies of the Lowest Excited Singlet States of Violaxanthin and Zeaxanthin†

Harry A. Frank,*,‡ James A. Bautista,‡ Jesusa S. Josue,‡ and Andrew J. Young§

*Department of Chemistry, U-60, University of Connecticut, 55 North Eagleville Road, Storrs, Connecticut 06269-3060, and School of Biological and Earth Sciences, Liverpool John Moores University, Liverpool L3 3AF, U.K.*

*Received October 22, 1999; Revised Manuscript Received December 16, 1999*

ABSTRACT: The xanthophyll cycle is an enzymatic, reversible process through which the carotenoids violaxanthin, antheraxanthin, and zeaxanthin are interconverted in response to the need to balance light absorption with the capacity to use the energy to drive the reactions of photosynthesis. The cycle is thought to be one of the main avenues for safely dissipating excitation energy absorbed by plants in excess of that needed for photosynthesis. One of the key factors needed to elucidate the molecular mechanism by which the potentially damaging excess energy is dissipated is the energy of the lowest excited singlet ($S_1$) state of the xanthophyll pigments. Absorption from the ground state ($S_0$) to $S_1$ is forbidden by symmetry, making a determination of the $S_1$ state energies of these molecules by absorption spectroscopy very difficult. Fluorescence spectroscopy is potentially the most direct method for obtaining the $S_1$ state energies. However, because of problems with sample purity, low emission quantum yields, and detection sensitivity, fluorescence spectra from these molecules, until now, have never been reported. In this work these technical obstacles have been overcome, and $S_1 \rightarrow S_0$ fluorescence spectra of violaxanthin and zeaxanthin are presented. The energies of the $S_1$ states deduced from the fluorescence spectra are 14 880 ± 90 $cm^{-1}$ for violaxanthin and 14 550 ± 90 $cm^{-1}$ for zeaxanthin. The results provide important insights into the mechanism of nonphotochemical dissipation of excess energy in plants.

When green plants are exposed to light levels in excess of those necessary for photosynthesis, nonphotochemical dissipation of the excess thermal energy occurs. This process, generically referred to as nonphotochemical quenching (NPQ)[1] (*1*, *2*), represents an adaptation by plants to environmental changes and provides protection of the photosynthetic apparatus against photoinduced damage. The safe removal of excess excitation energy within the chlorophyll (Chl) pigment bed is thought to be regulated by an enzymatic, reversible process involving the interconversion of the xanthophylls, violaxanthin, antheraxanthin, and zeaxanthin, and known as the xanthophyll cycle (Figure 1) (*3*−*6*). Evidence for a correlation between excess energy dissipation and the xanthophyll cycle emerged from experiments demonstrating that when plants are transferred from conditions of limiting light to excess light, a substantial increase in the collective pool size of the xanthophyll-cycle pigments relative to Chl is seen (*7*). In addition to this long-term adaptation to the environmental change, it was observed that excess light induces the de-epoxidation of violaxanthin to zeaxanthin, and that the yield of Chl fluorescence emission was inversely correlated with the amount of zeaxanthin in the existing xanthophyll pool (*8*). From this observation it was proposed that zeaxanthin acts as a particularly effective quencher of excess excitation energy. The reconversion of zeaxanthin to violaxanthin is favored when the leaves are subsequently transferred back to limiting light levels. Evidence has also been presented that a low luminal pH within the membranes is required for energy dissipation (*9*, *10*). An obligatory role for zeaxanthin in NPQ, however, remains controversial, and the precise mechanism(s) by which energy dissipation occurs is not yet fully understood (*11*).

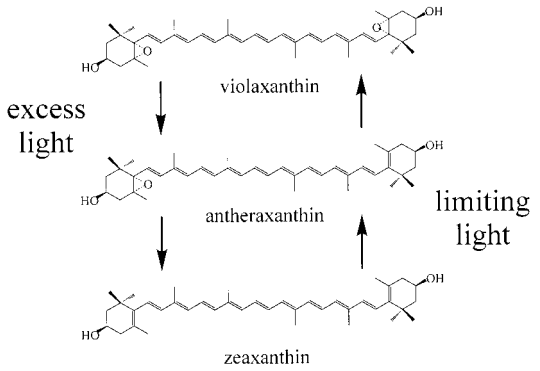


FIGURE 1: Schematic representation of the xanthophyll cycle showing the de-epoxidation of violaxanthin to zeaxanthin and the epoxidation of zeaxanthin to violaxanthin. Both of these reactions occur by way of antheraxanthin as an intermediate.

There have been two basic hypotheses to explain the role of zeaxanthin in NPQ: (i) *Direct quenching*. This model

† This work has been supported in part by the National Science Foundation (Grant MCB-9816759), the National Institutes of Health (Grant GM-30353), and the University of Connecticut Research Foundation.

* To whom correspondence should be addressed. Phone: (860) 486-2844. Fax: (860) 486-6558. E-mail: frank@uconnvm.uconn.edu.

‡ University of Connecticut.

§ Liverpool John Moores University.

[1] Abbreviations: Chl, chlorophyll; HPLC, high-performance liquid chromatography; NPQ, nonphotochemical quenching; PMT, photomultiplier tube.

10.1021/bi9924664 CCC: $19.00 
Published on Web 02/24/2000

proposes that downhill energy transfer from Chl *a* to zeaxanthin occurs after a pH-activated structural change in the pigment−protein complex facilitates the energy exchange (*8, 12, 13*). This idea has gained support from estimates of the energies of the lowest-lying singlet ($S_1$) states of the xanthophylls from either the dynamics or the fluorescence of a series of shorter carotenoids (less than 10 carbon−carbon double bonds), and extrapolation of the energies to the longer molecules including the pigments involved in the xanthophyll cycle (*13, 14*). The spectroscopic and kinetic investigations revealed that the energies of the $S_1$ states of the xanthophyll pigments are much lower than previously thought, and consequently may be low enough to quench Chl excited states. For a review of this topic see ref *15*. This could provide a means of regulating the flow of energy among pigments in the antenna. (ii) *Indirect quenching*. This model proposes that, upon binding to the protein, specific structural features possessed by the xanthophylls exert control over the organization of the pigments (xanthophylls and Chls) within the antenna complexes and lead to fluorescence quenching, or in some cases, antiquenching (*16*). Experiments carried out on isolated complexes have supported this hypothesis and have shown that zeaxanthin promotes aggregation of antenna complexes whereas violaxanthin has the opposite effect. It has also been argued that carotenoids other than zeaxanthin may also be effective in promoting aggregation that would result in the quenching of Chl fluorescence in vivo (*17*). In point of fact, however, neither the direct nor indirect quenching mechanisms have been demonstrated unequivocally in vivo.

Violaxanthin, zeaxanthin, and all xanthophylls display very strong absorption in the visible region. This absorption is associated with an electronic transition between the ground state, $S_0$, which has $A_g$ symmetry in the idealized $C_{2h}$ point group, and an excited singlet state which has $B_u$ symmetry and an energy higher than that of the lowest excited singlet state, $S_1$. This higher energy state is denoted $1^1B_u$. Electronic transitions between the ground state and $S_1$ are forbidden because these two states have the same ($A_g$) symmetry. Although there is some evidence that additional $A_g$ states lie near the $S_1$ ($2^1A_g$) and the $1^1B_u$ states in long polyenes and carotenoids (*18, 19*), the latter is usually referred to as $S_2$ because it is the most easily observed and spectroscopically accessible state above $S_1$.

The extremely low fluorescence yields of xanthophylls and carotenoids have made it difficult to detect and characterize their lowest excited singlet states, especially the $S_1$ state into which absorption is forbidden by symmetry. $\beta$-Carotene, spheroidene, and many other carotenoids have $S_2$ state fluorescence yields of $10^{-4}$ or less (*20*−*30*), and until recently (*26, 31, 32*), no reports of $S_1$ fluorescence from carotenoids having more than nine conjugated carbon−carbon double bonds had been published. The profound importance of fluorescence spectroscopy in detecting and understanding the nature of the lowest energy $S_1$ states of these molecules cannot be overemphasized.

A key factor in evaluating the viability of the mechanisms that have been proposed to explain NPQ is the energy of the $S_1$ states of the xanthophylls violaxanthin and zeaxanthin. These states undoubtedly play a major role in either light-harvesting or fluorescence quenching or both. The general difficulty in observing $S_1$ emission from carotenoids having more than nine carbon−carbon double bonds can be attributed to several factors including their broad, almost featureless emission profiles, very low ($\sim 10^{-6}$) fluorescence quantum yields, and unfortunate position on the long-wavelength tail of the relatively stronger $S_2$ emission. All of these factors have hindered what would be the most direct observation of the $S_1$ states of these molecules using fluorescence spectroscopic methods.

In previous work (*13*), the $S_1$ energy levels of the xanthophyll-cycle pigments were determined indirectly by measuring the dynamics of shorter carotenoids which exhibit fluorescence from their $S_1$ states, and then using the energy gap law for radiationless transitions to deduce the state energies (*33*−*35*). The energies determined in this manner were 15 290, 14 720, and 14 170 $cm^{-1}$ for violaxanthin, antheraxanthin, and zeaxanthin, respectively. Polívka et al. (*36*) reported a more direct method for obtaining the $S_1$ state energies of these molecules using femtosecond transient absorption spectroscopy of the $S_1 \rightarrow S_2$ transitions. These authors used the difference between the spectral origins of the transient $S_1 \rightarrow S_2$ bands and the strongly allowed $S_0 \rightarrow S_2$ absorption bands to deduce the $S_1$ state energies of the carotenoids. These authors reported $S_1$ energies of 14 470 $\pm$ 90 $cm^{-1}$ for violaxanthin and 14 030 $\pm$ 90 $cm^{-1}$ for zeaxanthin.

In this paper we present a direct determination of the $S_1$ energies of violaxanthin and zeaxanthin using fluorescence spectroscopy. The technical obstacles prohibiting the observation of $S_1$ fluorescence from the xanthophylls have been overcome by a combination of state-of-the art high-performance liquid chromatography (HPLC) to obtain ultrapure samples free of fluorescing impurities, laser excitation for efficient and stable optical pumping, photon counting to enhance the sensitivity of the detection of the weak emission, and Gaussian deconvolution of the emission bands to reveal the spectral origins of the lineshapes. The values of the $S_1$ energies deduced from these experiments are 14 880 $\pm$ 90 $cm^{-1}$ for violaxanthin and 14 550 $\pm$ 90 $cm^{-1}$ for zeaxanthin. Because of the vanishing small transition dipole moment associated with the $S_0 \rightarrow S_1$ transition of carotenoids, these values are likely to be very close to the energies of these molecules in vivo. This also assumes that no significant shifting of the $S_1$ states is caused by mixing with states from Chls in close proximity. The differences between the values measured here and those obtained by other techniques and the implications for the mechanism of NPQ will be discussed.

## MATERIALS AND METHODS

*Sample Preparation*. The xanthophylls were extracted from spinach leaves. Approximately 200 g of young spinach leaves was ground and mixed with ~500 mL of 70/30 v/v acetone/methanol mixture. The mixture was filtered, and the acetone/methanol pigment extract was evaporated on a rotary evaporator. The extract was dissolved in ~10 mL of 90/10 v/v methanol/diethyl ether mixture and saponified in a 6% w/v KOH, flushed with nitrogen, stoppered, and placed in the dark overnight at room temperature. The carotenoids were extracted using diethyl ether, dried with a gentle stream of $N_2$ gas in the dark, and redissolved in acetone. The saponified extracts were then injected into a Millipore Waters 600E HPLC employing a Nova-Pak $C_{18}$ column with the mobile

phase A = 9/1 v/v acetonitrile/water with 0.1% triethylamine and B = ethyl acetate. The run was programmed as follows: 0−16 min, linear gradient from 100% to 40% A; 16−40 min, isocratic 40% A with a flow rate of 1.0 mL/min. The fraction of the eluant containing violaxanthin was identified by its absorption spectrum on the model 996 diode array detector, collected, and dried with a gentle stream of $N_2$ gas as described above.

Zeaxanthin was purified by HLPC using the same solvent system as for violaxanthin, but with the mobile phase programmed as follows: 0−14 min, isocratic 100% A; 15−19 min, linear gradient to 77% A; 20−24 min, linear gradient to 30% A; 25−40 min, isocratic 100% B with a flow rate of 0.50 mL $min^{-1}$. The fraction of the eluant containing zeaxanthin was identified by its absorption on the diode array, collected, and dried under a steady stream of gaseous $N_2$. The samples were used in the fluorescence experiments immediately after purification by HPLC.

*Spectroscopic Methods*. *Steady-State Absorption and Fluorescence*. Absorption spectra were recorded at room temperature using a Milton Roy Spectronic 3000 Array photodiode array spectrometer. Fluorescence spectroscopy was carried out at 12 °C using an SLM Instruments, Inc. model 8000C spectrofluorimeter equipped with an emission monochromator with a grating of 1500 grooves/mm and a Hamamatsu R928 photomultiplier tube (PMT) as a detector. To minimize the PMT dark current, an SLM Instruments model WCTS-1 thermostatically cooled housing was used to lower the temperature of the PMT to ∼−20 °C.

A Spectra-Physics argon ion laser model 164 operating at a power of ∼50 mW was used to excite the molecules. A 470 nm long-pass cutoff filter was placed between the sample and the emission monochromator which was positioned 90° to the excitation beam. To obtain emission from both the $S_2$ and $S_1$ states of the molecules in a single sweep over the wavelength range 460−850 nm, the laser excitation was tuned to 454 nm. The SLM Aminco 8100 version 4.0 operating system software then automatically selected either signal-averaging or integration, whichever gave the better signal-to-noise ratio. The emission spectrum was then scanned at a relatively low amplifier gain and PMT voltage (∼700 V) to obtain the maximum signal intensity that would occur in that spectral range. The wavelength at which the maximum signal was observed was used by software to automatically set the PMT voltage and amplifier gain to achieve a signal that registered 80% of the saturation maximum of the PMT. The spectrum was then scanned again using these instrumental parameters, and afterward, a solvent blank was run under the same experimental conditions. The spectral scan of the solvent blank was subtracted from the spectral trace of the sample to remove contributions from Raman scattering from the solvent. The integrity of the samples was checked by HPLC after the laser excitation. No degradation of the samples was evident.

To enhance the observation of the $S_1$ emission, the laser was tuned to 476 nm and the power increased to ∼70 mW. The fluorescence spectrometer acquisition mode was then set to photon counting, which improved the signal-to-noise ratio of the very weak $S_1$ emission signals by a factor of between 2 and 5 compared to when the signal-averaging or integration modes were used. A 550 nm long-pass cutoff filter was placed between the sample and the emission monochomator, and the start wavelength for the emission spectrum was set at 620 nm to avoid saturating the PMT with the relatively more intense $S_2$ signals. Once again, contributions resulting from Raman scattering of the solvent were removed from the spectra by subtracting a scan of a solvent blank taken under identical conditions. Ideally, fluorescence excitation spectra should be taken to confirm that the emission from the samples is attributable to the xanthophylls and correlated with their absorption spectra. Unfortunately, this was precluded by the absolute necessity to use direct laser excitation of the samples to obtain acceptable signal-to-noise ratios in the emission spectra. The argon ion laser provided a profoundly more stable, high-intensity light source than any of our arc lamps with which excitation spectra, in principle, could have been taken. All of the fluorescence spectra presented here were corrected for the wavelength dependences of the optical components using a correction factor curve generated from a scan using a Spectral Irradiance 45 W quartz−halogen tungsten coiled filament lamp standard.

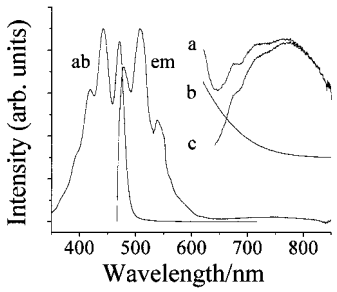


FIGURE 2: Absorption (ab) and fluorescence (em) spectra of violaxanthin in *n*-hexane. The absorption spectrum was taken at room temperature, and the fluorescence spectrum was taken at 12 °C. The absorption (ab) corresponds to the $S_0$ ($1^1A_g$) → $S_2$ ($1^1B_u$) transition. The most prominent feature in the emission (em) corresponds to the relatively strong $S_2$ ($1^1B_u$) → $S_0$ ($1^1A_g$) fluorescence taken using ∼50 mW of argon ion laser excitation at 454 nm. (a) $S_1$ ($2^1A_g$) → $S_0$ ($1^1A_g$) emission spectrum taken using ∼70 mW of argon ion laser excitation at 476 nm and the higher instrument sensitivity as described in the text. The spectra labeled em and a were corrected for the instrument response. (b) Gaussian fit to the tail of the $S_2$ ($1'B_u$) → $S_0$ ($1'A_g$) spectrum. (c) Difference between curves a and b showing more clearly the vibronic features of the $S_1$ ($2^1A_g$) → $S_0$ ($1^1A_g$) emission band.

*Computational Methods*. *Gaussian Deconvolutions*. The instrument-corrected fluorescence spectra were mathematically corrected for the effect of transforming the data from the fixed band-pass wavelength scale experiment to a nonlinear band-pass wavenumber scale. This was done by multiplying the experimental fluorescence intensities at each point by the square of the detection wavelength (*37*). Gaussian deconvolutions of the lineshapes were performed using Origin version 6.0 software as described below (*38*).

## RESULTS AND DISCUSSION

The $S_0$ → $S_2$ absorption and the $S_2$ → $S_0$ emission spectra from violaxanthin and zeaxanthin in *n*-hexane are shown in Figures 2 and 3, respectively. In both cases the $S_0$ → $S_2$ absorption spectra have approximate mirror-image symmetry with the $S_2$ → $S_0$ fluorescence spectra. The absorption and fluorescence spectra from zeaxanthin are slightly red-shifted compared to those from violaxanthin. This is due to the larger number of conjugated carbon−carbon double bonds pos-

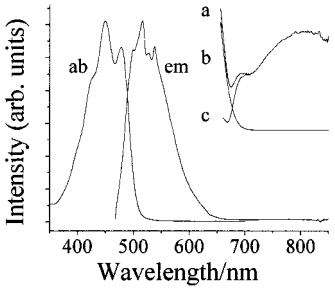


FIGURE 3: Absorption (ab) and fluorescence (em) spectra of zeaxanthin in *n*-hexane. The conditions for ab, em, a, b, and c were identical to those described for violaxanthin in the caption of Figure 2.

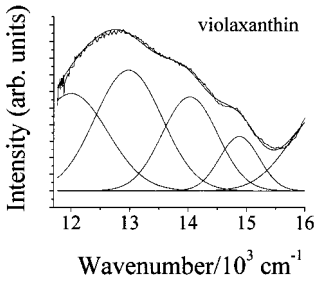


FIGURE 4: Gaussian deconvolution of the $S_1$ ($2^1A_g$) → $S_0$ ($1^1A_g$) emission spectrum of violaxanthin plotted on a wavenumber scale as described in the text. The parameters corresponding to the fit are given in Table 1.

sessed by zeaxanthin (11 conjugated carbon−carbon double bonds) compared to violaxanthin (9 conjugated carbon−carbon double bonds). See Figure 1. As is typically observed for carotenoids, the second vibronic feature represents the Franck−Condon maximum in the $S_0 \rightarrow S_2$ absorption and $S_2 \rightarrow S_0$ fluorescence spectra from both molecules (*39*). The spectral traces from violaxanthin show a higher degree of resolution in vibronic bands than those from zeaxanthin. This may be explained by the fact that the epoxide functional groups present in violaxanthin uncouple the isoprenoid rings from the $\pi$-electron conjugation, leading to less conformational disorder in the conjugated chain compared to carotenoids that have the rings in conjugation (*40*). The small sharp peaks near the emission maximum of zeaxanthin are Raman lines resulting from the laser excitation (*26*).

The $S_1 \rightarrow S_0$ fluorescence spectra from violaxanthin and zeaxanthin are shown in Figures 2a and 3a, respectively. In both cases the $S_1 \rightarrow S_0$ bands appear on the falling red edges of the respective $S_2 \rightarrow S_0$ emissions, although the $S_1$ emission from violaxanthin appears slightly closer to the $S_2$ emission than does that from zeaxanthin. The maximum in the $S_1$ emission spectrum from zeaxanthin appears at longer wavelength than that of violaxanthin, due to the longer extent of $\pi$-electron conjugation of zeaxanthin compared to violaxanthin. Figures 2c and 3c show the effect of subtracting single Gaussian tails (Figures 2b and 3b), fitted to the $S_2 \rightarrow S_0$ emission curves in the region 600−850 nm, from the instrument-corrected spectra shown in Figures 2a and 3a. Vibronic features are clearly evident in the $S_1$ emission spectra for both molecules.

Figures 4 and 5 show the instrument-corrected experimental spectra presented in Figures 2a and 3a replotted on a wavenumber scale. The spectra in Figures 4 and 5 were also corrected for the variable band-pass as described in the Materials and Methods. The $S_1 \rightarrow S_0$ emission spectra were

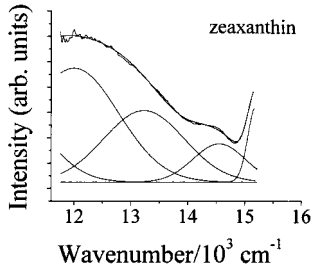


FIGURE 5: Gaussian deconvolution of the $S_1$ ($2^1A_g$) → $S_0$ ($1^1A_g$) emission spectrum of zeaxanthin plotted on a wavenumber scale as described in the text. The parameters corresponding to the fit are given in Table 1.

then simulated as follows: The starting values of the wavenumber positions of the vibronic bands were taken from the locations of the peaks and shoulders in the experimental spectra, and on the assumption that the spacings of the vibrational peaks should be roughly equidistant. In the first fitting calculation, all of the parameters, position, width, area, and spacing, were allowed to vary using a maximum of 100 iterations of the Levenberg−Marquardt algorithm. Constraints were then imposed on the widths of the Gaussians so that no vibronic band could take on more than double the width of an adjacent Gaussian band. Then another set of iterations was performed with the baseline set to a constant value. After this, the locations of the peaks were fixed according to the results of this last set of iterations, and then only the widths and areas of adjacent and nonadjacent Gaussians, respectively, were allowed to vary, keeping all other parameters constant. Finally, the parameters of each of the Gaussian bands were manually fine-tuned to finalize the fit. The final parameters for the fits are given in Table 1.

The Gaussian deconvolutions of the $S_1 \rightarrow S_0$ spectra revealed regular patterns of spectral lines representing normal vibronic band progressions, with the $0 \rightarrow 0$ band in both cases being the narrowest vibronic feature. This is typical of carotenoid and polyene spectra (*39*). The spectra display vibronic spacings in the range of 850−1320 cm$^{-1}$, with the spacings and widths of the vibronic bands associated with zeaxanthin being slightly larger than those for violaxanthin. (See Table 1.) This is most likely attributed to more conformational disorder in the conjugated $\pi$-electron system of zeaxanthin compared to violaxanthin as discussed above (*40*). Four Gaussian functions were needed to reproduce the observed spectral traces of both violaxanthin and zeaxanthin. These represent the $0 \rightarrow 0$, 1, 2, 3 vibronic bands of the $S_0 \rightarrow S_1$ emission spectra of both violaxanthin and zeaxanthin. In both cases the $0 \rightarrow 0$ spectral origins are clearly identified as the lowest energy vibronic component. The $0 \rightarrow 2$ component is the Franck−Condon maximum. This is typical of shorter carotenoids which display stronger $S_1$ emission than observed from these xanthophylls (*41*−*44*). The present data reveal the $0 \rightarrow 0$ spectral origins for the $S_1 \rightarrow S_0$ transitions of violaxanthin and zeaxanthin to be 14 880 ± 90 and 14 550 ± 90 cm$^{-1}$, respectively.

It is important to compare these values with those deduced from previous studies on similarly conjugated systems. Zeaxanthin is electronically isomorphous with $\beta$-carotene whose $S_1$ energy has been determined by fluorescence spectroscopy to be 14 500 cm$^{-1}$ in *n*-hexane and in single crystals (*45*, *46*) and 14 200 ± 500 cm$^{-1}$ in $CS_2$ (*31*). These

Table 1: Fitting Parameters for the Gaussian Deconvolutions of the $S_1$ ($2^1A_g$) → $S_0$ ($1^1A_g$) Emission Spectra of Violaxanthin and Zeaxanthin Given in Figures 4 and 5, Respectively[a]

| | | $S_1$ ($2^1A_g$) → $S_0$ ($1^1A_g$) | | | | $S_2$ ($1^1B_u$) → $S_0$ ($1^1A_g$) |
|---|---|---|---|---|---|---|
| | | 0 → 0 | 0 → 1 | 0 → 2 | 0 → 3 | 0 → 4 |
| violaxanthin | position ($cm^{-1}$) | 14 880 | 14 030 | 12 980 | 12 000 | 16 340 |
| | width ($cm^{-1}$) | 680 | 950 | 1150 | 1250 | 1200 |
| | area | $2.8 \times 10^{12}$ | $6.8 \times 10^{12}$ | $1.0 \times 10^{13}$ | $9.2 \times 10^{12}$ | $7.3 \times 10^{12}$ |
| zeaxanthin | position ($cm^{-1}$) | 14 550 | 13 230 | 12 000 | 10 900 | 15 200 |
| | width ($cm^{-1}$) | 910 | 1410 | 1570 | 1300 | 300 |
| | area | $3.4 \times 10^{13}$ | $1.0 \times 10^{14}$ | $1.8 \times 10^{14}$ | $8.9 \times 10^{13}$ | $2.3 \times 10^{13}$ |

[a] The fitting procedure was carried out as described in the text. The assignment of the 0 → 4 vibronic band in the $S_2$ ($1^1B_u$) → $S_0$ ($1^1A_g$) emission spectrum is based on the vibronic assignment of $\beta$-carotene by Koyama et al. (*45*).

values are in complete agreement with the value of 14 550 ± 90 $cm^{-1}$ obtained here. Using transient $S_1 \rightarrow S_2$ absorption spectroscopy, Polívka et al. (*36*) deduced a value of 14 030 ± 90 $cm^{-1}$ for the $S_1$ energy of zeaxanthin and 14 470 ± 90 $cm^{-1}$ for violaxanthin. These values are approximately 450 $cm^{-1}$ lower than those obtained here and appear to be outside the uncertainties of the two different types of measurements. However, the value of 14 470 $cm^{-1}$ obtained for violaxanthin by Polívka et al. (*36*) is significantly lower than those of other carotenoids possessing nine conjugated carbon−carbon double bonds. Fujii et al. (*26*) and DeCoster et al. (*14*) reported a value of 15 300 $cm^{-1}$ for the $S_1$ energies of neurosporene and methoxyneurosporene, respectively, which have nine conjugated carbon−carbon double bonds. Violaxanthin possesses two $C_{5,6}$ epoxidated rings and a symmetric electronic distribution along the carbon skeleton. In contrast, neurosporene and methoxyneurosporene are acyclic molecules in which the extent of conjugation is offset from the geometric center of the carbon skeleton. These structural differences could lead to differences in the positions of the $S_1$ energies of the neurosporene compounds compared to violaxanthin.

Although Polívka et al. (*36*) observe slightly lower values for the $S_1$ energies of zeaxanthin and violaxanthin compared to those reported here, the difference between the values of the $S_1$ energies for the two molecules (~400 $cm^{-1}$) is the same in the two studies. This suggests that there may be a systematic difference in the process of determining spectral origins from transient absorption methods compared to steady-state fluorescence spectroscopy. Also, the $S_1$ ($2^1A_g$) → $S_2$ ($1^1B_u$) transient absorption spectra of Polívka et al. (*36*) show a complex pattern of vibronic features, some of which have yet to be assigned. These could hold the key to understanding the small disparity in the results obtained from the two different methods.

Despite the minor discrepancies noted above, the results presented here and those of Polívka et al. (*36*) clearly show that the $S_1$ energies of violaxanthin and zeaxanthin are much closer to each other, i.e., within ~400 $cm^{-1}$, than previously thought on the basis of measurements of the dynamics of the $S_1$ states and using the energy gap law for radiationless transitions to obtain the energies. The previous analysis was based on a limited set of dynamics data and deduced the difference to be on the order of ~1000 $cm^{-1}$ (*34*, *35*). The question then is whether a ~400 $cm^{-1}$ difference in the $S_1$ energies of violaxanthin and zeaxanthin is sufficient to alter the flow of energy among Chl molecules in antenna systems containing the xanthophyll cycle pigments. On the basis of the maximum absorption of the Chl $Q_y$ transition at 672 nm in the light-harvesting complexes of higher plants, the $S_0 \rightarrow S_1$ ($Q_y$) transition energy of Chl *a* is 14 880 $cm^{-1}$. This is isoenergetic with the $S_1$ energy of violaxanthin determined here. It must be emphasized, however, that these excited-state energies are not absolute thresholds determining whether forward or reverse energy transfer can occur to or from Chl *a*. In assessing the extent to which either of these molecules may be more adept at performing either light-harvesting (forward energy transfer) or quenching of Chl excited singlet states (reverse energy transfer), it is appropriate to examine the relative magnitudes of the spectral overlap between the absorption and emission bands of the molecules. This is an important controlling factor in determining the rate of energy transfer between the molecules.

The transitions to and from the $S_0$ and the $S_1$ states of the xanthophylls involve transitions that are forbidden by symmetry. Hence, the appropriate spectral overlap integral derives from the Dexter formalism (*47*), where the rate constant for energy transfer is given by

$$k_{ET} = K \exp\left(\frac{-2r}{L}\right) J_{exchange} \quad (1)$$

*K* depends on the specific orbitals involved, *r* describes the donor−acceptor distance relative to their van der Waals radii, *L*, and $J_{exchange}$ is the overlap integral given by

$$J_{exchange} = \frac{\int_{-\infty}^{\infty} F_d(\nu)\, \epsilon_a(\nu) \nu^{-4}\, d\nu}{\int_{-\infty}^{\infty} F_d(\nu)\, d\nu \int_{-\infty}^{\infty} \epsilon_a(\nu)\, d\nu} \quad (2)$$

$F_d(\nu)$ is the emission spectral line shape function of the donor, $\epsilon_a(\nu)$ describes the absorption spectral line shape for the acceptor, and $\nu$ is the spectral frequency. It is important to mention that this same term is contained in models invoking higher order multipolar interactions to explain the mechanism of energy transfer between carotenoids and chlorophylls (*48*, *49*). The present data provide a direct observation of the $S_1 \rightarrow S_0$ emission from which the spectral overlap integrals between Chl *a* and zeaxanthin or violaxanthin may be evaluated. The magnitudes of the spectral overlap terms were calculated according to eq 2 from the $S_1 \rightarrow S_0$ emission spectrum of the xanthophyll and the absorption line shape of Chl *a*. (See Figure 6.) For the process of reverse energy transfer, i.e., the quenching of Chl *a* excited singlet states by the xanthophylls, the emission spectra of the xanthophylls were reflected about their spectral origins to give approximations to the $S_0 \rightarrow S_1$ absorption profiles for the molecules. The $J_{exchange}$ value corresponding to the

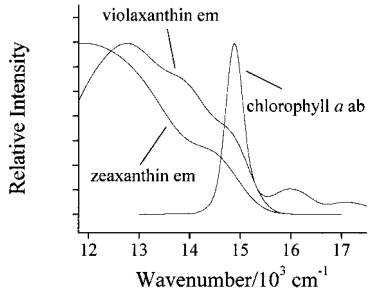


FIGURE 6: $S_1$ ($2^1A_g$) → $S_0$ ($1^1A_g$) emission traces for violaxanthin and zeaxanthin generated from the Gaussian fits overlaid with the absorption spectrum of Chl *a* for the purpose of calculating spectral overlaps according to eq 2 given in the text. This term contributes to the rate of energy transfer from the xanthophylls to Chl as shown by eq 1.

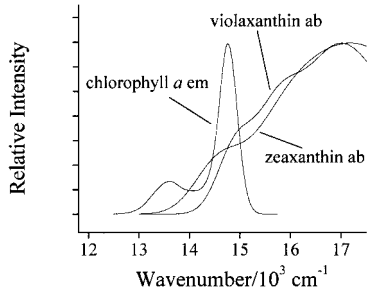


FIGURE 7: Hypothetical $S_0$ ($1^1A_g$) → $S_1$ ($2^1A_g$) absorption spectra of violaxanthin and zeaxanthin generated by reflecting the Gaussian fits to the emission traces given in Figure 6 about their spectral origins. The spectra are overlaid with the emission spectrum of Chl *a* for the purpose of calculating spectral overlaps according to eq 2 given in the text.

transfer of energy from Chl *a* to the carotenoid was then determined using eq 2 and the fluorescence spectrum of Chl *a*. (See Figure 7.) The ratio of the overlap integrals for the two xanthophylls carrying out forward energy transfer reveals that violaxanthin is predicted to be 2.1 ± 0.2 times more able to transfer energy from its $S_1$ state to Chl *a* than zeaxanthin (Figure 6). For the reverse process of Chl *a* fluorescence quenching by the two xanthophylls, the ratio of the overlap integrals was calculated to be 1.0 ± 0.2, indicating that, on the basis of energy levels alone, Chl *a* is predicted to have no more propensity to transfer energy to zeaxanthin than it does to violaxanthin. Although the spectral origin of Chl *a* lies between the spectral origins of zeaxanthin and violaxanthin, because of the broadness of the $S_1$ → $S_0$ and $S_0$ → $S_1$ spectral line shapes, both forward (light-harvesting) and reverse (quenching) energy-transfer processes between xanthophyll and Chl *a* are highly probable.

The present results show that direct quenching of chlorophyll fluorescence by violaxanthin and zeaxanthin is energetically feasible. However, because the energy difference between the $S_1$ states of zeaxanthin and violaxanthin is not large, differential quenching is unlikely to be controlled solely by energies of the $S_1$ states of the xanthophylls. This was also the conclusion of Polívka et al. (*36*). Hence, if the enzymatic de-epoxidation/epoxidation reactions of the xanthophyll cycle are to regulate energy flow in the pigment−protein complexes, then other factors, such as a *trans*-thylakoid pH gradient, phosphorylation, the involvement of other xanthophylls including lutein and antheraxanthin (*50*, *51*), and/or effects on the organization and structure of the light-harvesting complex, must be important in controlling this action.

## ACKNOWLEDGMENT

We thank Drs. Tomás Polívka, Jennifer Herek, and Villy Sundström for valuable discussions.

## REFERENCES

1. Horton, P., and Bowyer, J. R. (1990) in *Methods in Plant Biochemistry* (Harwood, J. L., and Bowyer, J. R., Eds.) Vol. 4, pp 259−296, Academic Press, London.
2. Krause, G. H., and Weis, E. (1992) *Annu. Rev. Plant Physiol. Mol. Biol. 42*, 313−349.
3. Sapozhnikov, D. I., Krasovskaya, T. A., and Mayevskaya, A. N. (1957) *Dokl. Akad. Nauk 113*, 456−467.
4. Hager, A. (1980) in *Pigments in Plants* (Czygan, F. C., Ed.) pp 57−79, Fischer, Stuttgart.
5. Yamamoto, H. Y. (1979) *Pure Appl. Chem. 51*, 639−648.
6. Yamamoto, H. Y., and Higashi, R. M. (1972) *Biochim. Biophys. Acta 267*, 538−543.
7. Demmig-Adams, B., Gilmore A. M., and Adams, W., III (1996) *FASEB J. 10*, 403−412.
8. Demmig-Adams, B. (1990) *Biochim. Biophys. Acta 1020*, 1−24.
9. Gilmore, A. M., and Yamamoto, H. Y. (1993) *Proc. Natl. Acad. U.S.A. 89*, 1899−1903.
10. Gilmore, A. M., and Yamamoto, H. Y. (1993) *Photosynth. Res. 35*, 67−78.
11. Niyogi, K. K., Björkman, O., and Grossman, A. R. (1997) *Proc. Natl. Acad. Sci. U.S.A. 94*, 14162−14167.
12. Owens, T. G., Shreve, A. V., and Albrecht, A. C. (1992) in *Research in Photosynthesis* (Murata, N., Ed.) Vol. 1, pp 179−186, Kluwer Academic Publishers, Dordrecht, The Netherlands.
13. Frank, H. A., Cua A., Chynwat, V., Young, A., Gosztola, D., and Wasielewski, M. R. (1994) *Photosynth. Res. 41*, 389−395.
14. DeCoster, B., Christensen, R. L., Gebhard, R., Lugtenburg, J., Farhoosh, R., and Frank, H. A. (1992) *Biochim. Biophys. Acta 1102*, 107−114.
15. Frank, H. A., and Christensen, R. L. (1995) Singlet Energy Transfer from Carotenoids to Bacteriochlorophylls, in *Anoxygenic Photosynthetic Bacteria*, *Advances in Photosynthesis* (Blankenship et al., Eds.) pp 373−384, Kluwer Academic Publishing, Dordrecht, The Netherlands.
16. Young, A. J., Phillip, D., Ruban, A. V., Horton, P., and Frank, H. A. (1997) *Pure Appl. Chem. 69*, 2125−2130.
17. Ruban, A. V., Phillip, D., Young, A. J., and Horton, P. (1998) *Photochem. Photobiol. 68*, 829−834.
18. Tavan, P., and Schulten, K. (1986) *J. Chem. Phys. 85*, 6602−6609.
19. Trautman, J. K., Owens, T. G., and Albrecht, A. C. (1990) *Chem. Phys. Lett. 170*, 51−56.
20. Petek, H., Bell, A. J., Kandori, H., Yoshihara, K., and Christensen, R. L. (1992) in *Time-resolved vibrational spectroscopy* (Takahashi, H., Ed.) Vol. 5, pp 198−199, Springer, Berlin.
21. Bondarev, S. L., Dvornikov, S. S., and Bachilo, S. M. (1988) *Opt. Spectrosc. (USSR) 64*, 268−270.
22. Bondarev, S. L., Bachilo, S. M., Dvornikov, S. S., and Tikhomirov, S. A. (1989) *J. Photochem. Photobiol. 46A*, 315−322.
23. Gillbro, T., and Cogdell, R. J. (1989) *Chem. Phys. Lett. 158*, 312−316.
24. Cosgrove, S. A., Guite, M. A., Burnell, T. B., and Christensen, R. L. (1990) *J. Phys. Chem. 94*, 8118−8124.
25. Desamero, R. Z. B., Chynwat, V., van der Hoef, I., Jansen, F. J., Lugtenburg, J., Gosztola, D., Wasielewski, M. R., Cua, A., Bocian, D. F., and Frank, H. A. (1998) *J. Phys. Chem. 42*, 8151.
26. Fujii, R., Onaka, K., Kuki, M., Koyama, Y., and Watanabe, Y. (1998) *Chem. Phys. Lett. 288*, 847−853.

27. Cherry, R. J., Chapman, D., and Langelaar, J. (1968) *Trans. Far. Soc. 64*, 2304−2307.
28. van Riel M., Kleinen-Hammans, J., van de Ven M., Verwer, W., and Levine Y. (1983) *Biochem. Biophys. Res. Commun. 113*, 102−107.
29. Haley, L. V., and Koningstein, J. A. (1983) *Chem. Phys. 77*, 1−9.
30. Watanabe, J., Kinoshita, S., and Kushida, T. (1986) *Chem. Phys. Lett. 126*, 197−200.
31. Andersson, P. O., Bachilo, S. M., Chen, R. L., and Gillbro, T. (1995) *J. Phys. Chem. 99*, 16199−16209.
32. Bondarev, S. L., and Knyukshto, V. N. (1994) *Chem. Phys. Lett. 225*, 346−350.
33. Englman, R., and Jortner, J. (1970) *Mol. Phys. 18*, 145−164.
34. Frank, H. A., Farhoosh, R., Gebhard, R., Lugtenburg, J., Gosztola, D., and Wasielewski, M. R. (1993) *Chem. Phys. Lett. 207*, 88−92.
35. Chynwat, V., and Frank, H. A. (1995) *Chem. Phys. 194*, 237−244.
36. Polívka, T., Herek, J. L., Zigmantas, D., Akerlund, H., and Sundström, V. (1999) *Proc. Natl. Acad. Sci. U.S.A. 96*, 4914.
37. Lakowicz, J. R. (1983) *Principles of Fluorescence Spectroscopy*, pp 67−70, Plenum Press, New York and London.
38. Microcal Software, Inc., One Roundhouse Plaza, Northampton, MA 01060.
39. Christensen, R. L., Goyette, M., Gallagher, L., Duncan, J., DeCoster, B., Lugtenburg, J., Jansen, F. J., and van der Hoef, I. (1999) *J. Phys. Chem. 103*, 2399−2407.
40. Christensen, R. L., and Kohler, B. E. (1973) *Photochem. Photobiol. 18*, 293−301.
41. Bautista, J. A., Hiller, R. G., Sharples, F. P., Gosztola, D., Wasielewski, M., and Frank, H. A. (1999) *J. Phys. Chem. 103A*, 2267−2273.
42. Katoh, T., Nagashima, U., and Mimuro, M. (1991) *Photosynth. Res. 27*, 221−226.
43. Mimuro, M., Nagashima, U., Takaichi, S., Nishimura, Y., Yamazaki, I., and Katoh, T. (1992) *Biochim. Biophys. Acta 1098*, 271−274.
44. Cosgrove, S. A., Guite, M. A., Burnell, T. B., and Christensen, R. L. (1990) *J. Phys. Chem. 94*, 8118−8124.
45. Koyama, Y., and Fujii, R. (1999) in *The Photochemistry of Carotenoids* (Frank, H. A., Britton, G., and Cogdell, R. J., Eds.) pp 161−188, Kluwer Academic Publishers, Dordrecht, The Netherlands.
46. Hashimoto, H., Koyama, Y., and Mori, Y. (1997) *Jpn. J. Appl. Phys. 36*, L916−L918.
47. Dexter, D. L. (1953) *J. Chem. Phys. 21*, 836−860.
48. Nagae, H., Kakitani, T., Katoh, T., and Mimuro, M. (1993) *J. Chem. Phys. 98*, 8012−8023.
49. Krueger, B. P., Scholes, G. D., Jimenez, R., and Fleming, G. R. (1998) *J. Phys. Chem. 102*, 2284−2292.
50. Horton, P., Ruban, A. V., Rees, D., Pascal, A. A., Noctor, G., and Young, A. J. (1991) *FEBS Lett. 292*, 1−4.
51. Horton, P., and Ruban, A. V. (1992) *Photosynth. Res. 34*, 375−385.

BI9924664